

Latitudinal change of remineralization ratios in the oceans and its implication for nutrient cycles

Yuan-Hui Li

Department of Oceanography, University of Hawaii, Honolulu, Hawaii, USA

Tsung-Hung Peng

NOAA/AOML, Ocean Chemistry Division, Miami, Florida, USA

Received 6 November 2001; revised 30 August 2002; accepted 5 September 2002; published 14 December 2002.

[1] A new three-end-member mixing model is introduced to obtain remineralization ratios of organic matter in the water column. Remineralization ratios ($P/N/C_{org}/-O_2$) of organic matter in the deep water column change systematically from the northern Atlantic to the Southern Oceans, then to the equatorial Indian and the northern Pacific oceans, more or less along the global ocean circulation route of deep water. Average remineralization ratios of organic matter for the northern Atlantic Ocean are $P/N/C_{org}/-O_2 = 1/(16 \pm 1)/(73 \pm 8)/(137 \pm 7)$, and for the Southern Oceans $P/N/C_{org}/-O_2 = 1/(15 \pm 1)/(80 \pm 3)/(133 \pm 5)$. Those values are similar to the traditional Redfield ratios of $P/N/C_{org}/-O_2 = 1/16/106/138$ for marine plankton, except for the low C_{org}/P ratio. Average remineralization ratios for the equatorial Indian Ocean are $P/N/C_{org}/-O_2 = 1/(10 \pm 1)/(94 \pm 5)/(130 \pm 7)$, and for the northern Pacific Ocean $P/N/C_{org}/-O_2 = 1/(13 \pm 1)/(124 \pm 11)/(162 \pm 11)$. The apparent low N/P ratio for both ocean basins suggests that organic nitrogen was converted partly into gaseous N_2O and N_2 by bacteria through nitrification/denitrification processes in a low-oxygen or reducing microenvironment of organic matter throughout the oxygenated water column. The actual N/P ratio of remineralized organic matter is probably around 15 ± 1 . The $-O_2/C_{org}$ ratio of remineralized organic matter also decreases systematically along the global ocean circulation route of deep water, indicating changes in relative proportions of biomolecules such as lipids, proteins, nucleic acids, and carbohydrates. No temporal trends of remineralization ratios are detected when comparing the results obtained by GEOSECS and WOCE data sets. **INDEX TERMS:** 4805 Oceanography: Biological and Chemical: Biogeochemical cycles (1615); 4806 Oceanography: Biological and Chemical: Carbon cycling; 4825 Oceanography: Biological and Chemical: Geochemistry; 4845 Oceanography: Biological and Chemical: Nutrients and nutrient cycling; **KEYWORDS:** remineralization ratios, nutrient cycles, global ocean circulation, latitudinal change, GEOSECS, WOCE

Citation: Li, Y.-H., and T.-H. Peng, Latitudinal change of remineralization ratios in the oceans and its implication for nutrient cycles, *Global Biogeochem. Cycles*, 16(4), 1130, doi:10.1029/2001GB001828, 2002.

1. Introduction to a New Three-End-Member Mixing Model

[2] Redfield [1958] proposed an idealized molar formula for an average marine plankton, i.e., $(CH_2O)_{106}(NH_3)_{16}(H_3PO_4)$. Oxidation or remineralization of one mole of this idealized plankton can be represented by the following overall net reaction: $(CH_2O)_{106}(NH_3)_{16}(H_3PO_4) + 138 O_2 \rightarrow 106 CO_2 + 16 NO_3^- + H_2PO_4^- + 17 H^+ + 122 H_2O$. Molar ratios among remineralized P, N, C_{org} , and consumed O_2 ($P/N/C_{org}/-O_2$) are called remineralization ratios or Redfield ratios. Remineralization ratios of $P/N/C_{org}/-O_2 = 1/16/106/138$ for the idealized marine plankton are known

as the “traditional Redfield ratios”. Remineralization ratios are useful in explaining the coupled nature of nutrients and carbon cycles in the oceans. They are also important constants needed to estimate conservative tracers such as “NO” and “PO” [Broecker, 1974; Broecker *et al.*, 1985]; the preformed nitrate, phosphate, and total dissolved inorganic carbon (NO_3^0 , PO_4^0 and DIC^0) [Chen and Pytkowicz, 1979; Li *et al.*, 2000]; and the extent of denitrification and nitrogen fixation [Gruber and Sarmiento, 1997; Deutsch *et al.*, 2001] in the oceans. It has been assumed that remineralization ratios remain constant over the global oceans. The availability of high quality data of nutrients and carbon chemistry as a result of WOCE/JGOFS global ocean survey provides an opportunity to reevaluate the remineralization ratios of organic matter and challenge the validity of their uniformity in the world oceans. Possible spatial and tem-

poral changes of remineralization ratios in the oceans are the subject of the present study.

[3] *Li et al.* [2000] presented a new two-end-member mixing model to estimate remineralization ratios $P:N:C_{org}:-O_2 = 1:(r_p/r_n):(r_p/r_c):r_p$. Here, r_p , r_n , and r_c are respectively the molar ratios of consumed O_2 to remineralized P, N, and C_{org} during oxidation of organic matter in the water column, i.e. $r_p = -O_2/P$, $r_n = -O_2/N$, and $r_c = -O_2/C_{org}$. The model essentially involves a multiple-variable linear regression (hereafter simplified as multiple regression) of hydrographic data of water samples within the linear segment of a chosen θ -S (potential temperature versus salinity) plot to obtain r_p , r_n , and r_c values. Hydrographic variables include potential temperature (θ), dissolved oxygen (O_2) along with dissolved inorganic phosphate (PO_4) or dissolved nitrate ($= NO_3^- + NO_2^-$), or DA ($= DIC - Alkalinity/2$). The advantage of this model over earlier ones [*Takahashi et al.*, 1985; *Broecker et al.*, 1985; *Minster and Boulahtid*, 1987; and *Boulahtid and Minster*, 1989] is that it requires no knowledge of the end-member values for each variable. As noted by *Minster and Boulahtid* [1987], the way end-member values were chosen in earlier models could be problematic. The model by *Anderson and Sarmiento* [1994] also requires no knowledge of end-member values. However, their assumption that ΔC_{inorg} (carbon increment from dissolution of carbonates) divided by ΔP (phosphate increment from oxidation of organic material) is constant along any neutral surface in their model is unrealistic, especially in water masses above the carbonate saturation depth. As summarized by *Morse and Mackenzie* [1990], the calcite saturation depth is about 4000 ± 500 m in the Indian and Pacific Oceans and 4500 ± 500 m in the Atlantic Ocean. In a saturated or oversaturated water mass, the formation processes of carbonates are completely decoupled from the oxidation process of organic matter. Only in some micro-environments may the oxidation of organic matter enhance the dissolution of carbonates [*Troy et al.*, 1997].

[4] *Hupe and Karstensen* [2000] introduced a linear inverse mixing model with multiple end-members to estimate remineralization ratios in the Arabian Sea. However, the model requires knowledge of end-member values for each variable. The choice of proper end-member characteristics is always subjective, especially for nonconservative tracers. *Shaffer* [1996] fitted global averaged profiles of phosphate, nitrate, and dissolved oxygen to his high-latitude-exchange/interior-diffusion-advection model to estimate remineralization ratios, and he concluded that remineralization ratios change with depth. Using a new diffusion-advection model with source or sink terms and allowing local exchange across neutral surfaces, *Shaffer et al.* [1999] obtained a similar conclusion but the remineralization ratios reach constant values below 1500 m. The model by *Shaffer et al.* [1999] also requires a prior knowledge of end-member characteristics. In contrast, *Broecker et al.* [1985], *Peng and Broecker* [1987], and *Anderson and Sarmiento* [1994] concluded that remineralization ratios do not change much with depth below 400 m.

[5] To use available data more effectively and to cover a greater portion of ocean regions for the evaluation of remineralization ratios, a logical extension of the two-end-

member mixing model of *Li et al.* [2000] is to introduce the additional conservative tracer salinity (S) and construct a three-end-member mixing model. In this model, selected data need not be confined in the linear segment of the θ -S diagram as required for any two-end-member mixing model. The model also requires no prior knowledge on the end-member values for each variable.

[6] The following mass balance equations for three conservative tracers, θ , S, and (NO), hold in a water sample that resulted from three-end-member mixing:

$$1 = f_1 + f_2 + f_3 \quad (1a)$$

$$\theta = f_1 \cdot \theta_1 + f_2 \cdot \theta_2 + f_3 \cdot \theta_3 \quad (1b)$$

$$S = f_1 \cdot S_1 + f_2 \cdot S_2 + f_3 \cdot S_3 \quad (1c)$$

$$O_2 + r_n \cdot NO_3 = (NO) = f_1 \cdot (NO)_1 + f_2 \cdot (NO)_2 + f_3 \cdot (NO)_3. \quad (1d)$$

Here θ , S, O_2 , and NO_3 are observed values for the water sample; subscripts 1, 2, and 3 represent the three end-members; f_i is the fraction of the end-member i ($= 1, 2,$ and 3) in the sample; $(NO)_i$ is the concentration of conservative tracer "NO" ($= O_2 + r_n \cdot NO_3$; here r_n is assumed constant [*Broecker*, 1974]) for the end-member i . First, we solve for f_1 , f_2 , and f_3 from equations (1a) to (1c) in terms of observed θ and S, and end-member values θ_i and S_i ; then substitute the solutions into equation (1d). The result is a linear equation:

$$O_2 = \alpha_0 + \alpha_1 \cdot \theta + \alpha_2 \cdot S - r_n \cdot NO_3 \quad (2a)$$

$$\begin{aligned} \text{Here } \alpha_0 &= [(\theta_2 S_3 - \theta_3 S_2)(NO)_1 + (\theta_3 S_1 - \theta_1 S_3)(NO)_2 \\ &\quad + (\theta_1 S_2 - \theta_2 S_1)(NO)_3] / D \\ \alpha_1 &= [(S_2 - S_3)(NO)_1 + (S_3 - S_1)(NO)_2 \\ &\quad + (S_1 - S_2)(NO)_3] / D \\ \alpha_2 &= [(\theta_3 - \theta_2)(NO)_1 + (\theta_1 - \theta_3)(NO)_2 \\ &\quad + (\theta_2 - \theta_1)(NO)_3] / D \\ D &= (\theta_2 S_3 - \theta_3 S_2) + (\theta_3 S_1 - \theta_1 S_3) + (\theta_1 S_2 - \theta_2 S_1). \end{aligned}$$

Note that the coefficients α_0 , α_1 , α_2 , and D are all functions of θ_i , S_i , and $(NO)_i$ ($i = 1, 2,$ and 3) for the three end-members, and are unknown but stay constant during the mixing process. One may regard end-member values θ_i , S_i , and $(NO)_i$ as mathematical dummies, and they need not have explicit values.

[7] By multiple regression of O_2 , θ , S and NO_3 concentration data from a properly selected hydrographic transect that contains three end-members (see the next section), one can estimate the regression coefficients α_0 , α_1 , α_2 , and r_n in equation (2a). However, our focus is only on the value of r_n . As discussed by *Li et al.* [2000], one can rewrite equation (2a) to make NO_3 a dependent variable, i.e.,

$$NO_3 = \alpha_0 / r_n + \alpha_1 / r_n \cdot \theta + \alpha_2 / r_n \cdot S - 1 / r_n \cdot O_2 \quad (2b)$$

[8] By multiple regression, one can also obtain independently $1/r_n$ and thus its inverse, designated here as r'_n . The r_n and r'_n values are always not equal, unless the square of the multiple correlation (R^2) is one. The results given in this paper are all averaged values, i.e., $(r_n + r'_n)/2$ with the estimated uncertainty of $\pm[(r_n - r'_n)/2]$ or $\pm[(\Delta r_n)^2 + (\Delta r'_n)^2]^{1/2}/2$, whichever is larger. Here, Δr_n and $\Delta r'_n$ are the standard errors for r_n and r'_n , given by any multiple regression program for personal computer (in our case, we used the Statistical Package for the Social Sciences, SPSS). When the square of the multiple correlation (R^2) is 0.98 or higher for the multiple regression, the r_n and r'_n values always overlap each other within the estimated standard errors.

[9] Similarly, replacing “NO” in equation (1d) with another conservative tracer “PO” ($= O_2 + r_p \cdot PO_4$ [Broecker, 1974]), and NO_3 with PO_4 , one obtains the following:

$$O_2 = A_0 + A_1 \cdot \theta + A_2 \cdot S - r_p \cdot PO_4 \quad (2c)$$

where A 's are similar in formula to α 's given beneath equation (2a), except replacing end-member values (NO)_{*i*} with (PO)_{*i*}. Again, by multiple regression of O_2 , θ , S , and PO_4 data, one can obtain r_p , r'_p and $(r_p + r'_p)/2$.

[10] When O_2 data are missing, the r_p/r_n ($= N/P$) ratio still can be estimated by multiple regression of NO_3 , θ , S , and PO_4 data according to the following equation, which is obtained by eliminating O_2 from equations (2a) to (2c):

$$NO_3 = (\alpha_0 - A_0)/r_n + (\alpha_1 - A_1)/r_n \cdot \theta + (\alpha_2 - A_2)/r_n \cdot S \\ + r_p/r_n \cdot PO_4, \text{ or}$$

$$PO_4 = (A_0 - \alpha_0)/r_p + (A_1 - \alpha_1)/r_p \cdot \theta + (A_2 - \alpha_2)/r_p \cdot S \\ + r_n/r_p \cdot NO_3 \quad (2d)$$

[11] As shown by *Li et al.* [2000], the following relationships are valid for total dissolved inorganic carbon (DIC) and total alkalinity (Alk) in a water sample:

$$x + y = DIC - DIC^0 \quad (3a)$$

$$2x - a \cdot y = Alk - Alk^0 \quad (3b)$$

$$r_c \cdot y = O_2^0 - O_2 \approx AOU \quad (3c)$$

where x and y are respectively cumulative increments of DIC from dissolution of carbonate minerals and from oxidation of organic matter during the transport of a water sample from its source region to the current position; “ a ” = H^+/C_{org} (molar ratio of the produced H^+ to the remineralized C_{org} during oxidation of organic matter) = $(N + P)/C_{org} = r_c/r_n + r_c/r_p \approx r_c/r_n$ (since $r_c/r_n \gg r_c/r_p$); DIC^0 , Alk^0 , and O_2^0 are the initial values at the source region. If O_2^0 is the saturated oxygen concentration at the given S and θ of the water sample in equilibrium with air, then $(O_2^0 - O_2)$ by definition becomes AOU (apparent oxygen utilization), and DIC^0 and Alk^0 are the preformed DIC and alkalinity.

[12] By assuming O_2^0 to be equal to the saturated oxygen in equilibrium with air, and eliminating x and y from equations (3a) to (3c), one obtains the following:

$$DIC - Alk/2 = DIC^0 - Alk^0/2 + [(a/2 + 1)/r_c] \cdot AOU, \\ \text{or simplified as}$$

$$DA = DA^0 + [(a/2 + 1)/r_c] \cdot AOU \quad (4a)$$

where $DA = DIC - Alk/2$, and $DA^0 (= DIC^0 - Alk^0/2)$ is the preformed DA .

[13] The new variable DA (combining capital letters of DIC and Alk) can be visualized as alkalinity-corrected DIC [Li et al., 2000]. Like any other preformed parameter, DA^0 is also a conservative tracer that changes in water samples only through water mass mixing before the industrial time. Strictly speaking, DA^0 is no longer a conservative tracer for the shallow part of the ocean where DIC^0 changes with time due to anthropogenic CO_2 inputs. However, the increment rate of DIC in the surface mixed layer is only about 0.05% per year [Winn et al., 1998]. Furthermore, the regionwide vertical mixing coefficient for the oceanic thermocline below the surface mixed layer is also finite (0.5 to 2.8 cm^2/s , which corresponds to 56 to 94 m of average mixing depth per year [Li et al., 1984]). Therefore, DA^0 still can be considered as near constant in the lower thermocline waters during a short period of one to five years, and it contains both the preindustrial and cumulative anthropogenic CO_2 components. DA^0 for any deep-water sample, where anthropogenic CO_2 input is negligibly small [Sarmiento et al., 1992; Wanninkhof et al., 1999], can be expressed by

$$DA^0 = f_1 \cdot DA_1^0 + f_2 \cdot DA_2^0 + f_3 \cdot DA_3^0 \quad (4b)$$

if the water sample is formed by three-end-member mixing.

[14] By substituting equations (1a), (1b), (1c) and (4b) into equation (4a), one obtains

$$DA = \beta_0 + \beta_1 \cdot \theta + \beta_2 \cdot S + \beta_3 \cdot AOU \quad (4c)$$

where β_0 , β_1 , and β_2 are similar in formula to α_0 , α_1 , and α_2 in equation (2a), except (NO)_{*i*} are replaced by (DA)_{*i*}; and $\beta_3 = (a/2 + 1)/r_c$, thus $r_c = 1/[\beta_3 - 0.5(1/r_n + 1/r_p)] \approx 1/[\beta_3 - 0.5/r_n]$. As will be shown in Table 1, the range of r_n is between 8 and 13, therefore the change in r_n will not affect the r_c value much. Again, one can estimate β_3 , thus r_c as well as r'_c and $(r_c + r'_c)/2$, by multiple regression of DA , θ , S , and AOU data for deep waters from lower thermocline and below, using equation (4c).

[15] One needs not assume O_2^0 to be equal to the saturated oxygen in equilibrium with air, and rewrite equation (4c) to

$$DA = \beta_0 + \beta_1 \cdot \theta + \beta_2 \cdot S + \beta_3 \cdot (O_2^0 - O_2) \quad (4d)$$

Substituting $O_2^0 = f_1 \cdot (O_2^0)_1 + f_2 \cdot (O_2^0)_2 + f_3 \cdot (O_2^0)_3$ into equation (4d), one obtains

$$DA = B_0 + B_1 \cdot \theta + B_2 \cdot S - \beta_3 \cdot O_2 \quad (4e)$$

Table 1a. Remineralization Ratios Based on the WOCE and GEOSECS Sections in the Atlantic Ocean^a

Section	Latitude Interval	Station Number	θ , °C	r_p ($-O_2/P$)	r_n ($-O_2/N$)	r_p/r_n (N/P)	β_3	r_c ($-O_2/C_{org}$)	r_p/r_c (C_{org}/P)
Redfield				138	8.6	16	0.83	1.30	106
a20	42°N–33.5°N	12–33	3–18	142 ± 2	8.6 ± 0.1	16.5 ± 0.3	0.66 ± 0.02	1.67 ± 0.06	85 ± 2
	33°N–13.5°N	34–63	3–6	132 ± 2	8.5 ± 0.2	15.5 ± 0.4	0.58 ± 0.04	1.93 ± 0.15	68 ± 2
			6–12	145 ± 3	8.7 ± 0.2	16.7 ± 0.5	0.62 ± 0.02	1.79 ± 0.07	81 ± 3
	13°N–7°N	64–92	3–5.2	140 ± 3	9.6 ± 0.3	14.6 ± 0.6	0.52 ± 0.02	2.15 ± 0.10	65 ± 2
a17	6°N–0°	175–235	4.2–12	125 ± 3	7.9 ± 0.1	15.8 ± 0.4	0.64 ± 0.01	1.75 ± 0.04	72 ± 2
	0°–25°S	88–174	4–12	140 ± 2	8.5 ± 0.1	16.5 ± 0.3	0.67 ± 0.01	1.65 ± 0.03	85 ± 2
	25°S–40°S	33–87	0.2–3	124 ± 3	8.0 ± 0.1	15.5 ± 0.4	0.74 ± 0.01	1.48 ± 0.03	84 ± 2
			3–12	127 ± 1	8.6 ± 0.1	14.8 ± 0.2	0.66 ± 0.01	1.67 ± 0.03	76 ± 1
	40°S–50°S	5–32	0.4–2.6	126 ± 4	8.5 ± 0.2	14.8 ± 0.6	0.74 ± 0.01	1.48 ± 0.03	85 ± 3
			2.6–12	126 ± 2	8.8 ± 0.2	14.3 ± 0.4	0.64 ± 0.01	1.73 ± 0.03	73 ± 2
	average			133 ± 8	8.6 ± 0.4	15.5 ± 0.8	0.65 ± 0.06	1.73 ± 0.19	77 ± 7
Geosecs	42°N–12°N	27–38	2–6	132 ± 5	7.9 ± 0.3	16.7 ± 0.9			
			6–18	127 ± 4	8.1 ± 0.2	15.7 ± 0.6			
	9°N–8°S	39–49	1.8–3.8	116 ± 1	8.9 ± 0.1	13.0 ± 0.2	0.70 ± 0.06	1.56 ± 0.15	74 ± 1
			3.8–12	120 ± 3	8.8 ± 0.1	13.6 ± 0.4	0.71 ± 0.04	1.54 ± 0.10	78 ± 2
	8.5°S–24°S	50–57	1.8–4	121 ± 2	9.0 ± 0.1	13.4 ± 0.3			
			3.2–12	133 ± 2	8.9 ± 0.1	14.9 ± 0.3	0.69 ± 0.02	1.59 ± 0.05	84 ± 2
	27°S–49°S	59–68	2.6–12	128 ± 1	9.0 ± 0.1	14.2 ± 0.2	0.71 ± 0.02	1.54 ± 0.05	83 ± 1
	average			126 ± 6	8.8 ± 0.6	14.5 ± 1.2	0.70 ± 0.01	1.55 ± 0.02	82 ± 5

^aNo bottom waters in the Atlantic Ocean were used in the model calculation, because the change of oxygen concentration in bottom waters can be explained solely by water mass mixing.

where constants B_0 , B_1 , and B_2 are bulky functions of θ_i^0 , S_i^0 , DA_i^0 , O_2^0 , for three end-members and β_3 .

[16] By multiple regression of DA , θ , S , and O_2 data using equation (4e), one can estimate β_3 , thus r_c , as well as r_c' and $(r_c + r_c')/2$. In practice, both equations (4c) and (4e) give the same β_3 values within the estimated uncertainty. Therefore, the assumption that O_2^0 represents the saturated oxygen in equilibrium with air is a good approximation.

[17] In short, the advantage of the present three-end-member model is that the data points selected for the model need not be confined in an isopycnal horizon [Takahashi *et al.*, 1985; Broecker *et al.*, 1985; Minster and Boulahdid, 1987] or neutral surface [Anderson and Sarmiento, 1994]. The data points can be expanded greatly (easily to more than one hundred to several hundreds data points for each run) to include those in a vertical cross section or in a large

volume of a given regional basin without having to worry about distinguishing horizontal/vertical or isopycnal/diapycnal mixing.

2. Steps in the Model Calculation

[18] To illustrate how these model calculations are conducted, we use the WOCE (World Ocean Circulation Experiment) hydrographic data from the transect p15 (roughly along the meridian 170°W) of the Pacific Ocean as an example. First, we grouped the stations in such a way that data points in a θ - S plot for a chosen latitudinal interval can be easily explained by mixing of three end-members. For example, in Figure 1a (stations 2 to 31 within latitudinal interval between 54°N and 41°N), data points with θ between 1° and 6°C (dotted horizontal lines) can be formed

Table 1b. Remineralization Ratios Based on the WOCE and GEOSECS Sections in the Indian Ocean^a

Section	Latitude Interval	Station Number	θ , °C	r_p ($-O_2/P$)	r_n ($-O_2/N$)	r_p/r_n (N/P)	β_3	r_c ($-O_2/C_{org}$)	r_p/r_c (C_{org}/P)
Redfield				138	8.6	16	0.83	1.30	106
i8N	6°N–0.5°S	279–303	1b–9	120 ± 3	13.0 ± 0.3	9.2 ± 0.3	0.79 ± 0.04	1.34 ± 0.07	90 ± 3
	0.5°S–18.5°S	304–343	0.9b–8	129 ± 2	12.6 ± 0.4	10.2 ± 0.4	0.78 ± 0.04	1.36 ± 0.07	95 ± 3
	19°S–29.5°S	344–393	2–8	129 ± 1	10.4 ± 0.1	12.4 ± 0.2	0.67 ± 0.03	1.62 ± 0.08	80 ± 1
	30°S–33°S	394–442	2–8	127 ± 2	10.4 ± 0.2	12.2 ± 0.3	0.69 ± 0.07	1.57 ± 0.17	81 ± 2
i8S	30°S–51°S	4–49	2–11	133 ± 3	9.5 ± 0.3	14.0 ± 0.5	0.66 ± 0.03	1.66 ± 0.08	80 ± 3
	51°S–63.5°S	50–84	*	130 ± 3	8.5 ± 0.2	15.3 ± 0.5	0.72 ± 0.03	1.52 ± 0.07	85 ± 3
i9N	20°N–2.5°N	213–277	0.8b–11	131 ± 1	13.0 ± 0.2	10.1 ± 0.2	0.77 ± 0.02	1.37 ± 0.04	95 ± 2
	2°N–18.5°S	172–212	0.8b–8	142 ± 1	13.4 ± 0.2	10.6 ± 0.2	0.76 ± 0.02	1.39 ± 0.04	102 ± 2
	19°S–31°S	148–171	2–10	134 ± 1	10.5 ± 0.2	12.8 ± 0.2	0.69 ± 0.01	1.57 ± 0.03	86 ± 1
i9S	34.5°S–50°S	114–147	2–11	152 ± 2	9.8 ± 0.2	15.5 ± 0.4	0.60 ± 0.05	1.83 ± 0.17	83 ± 2
	50°S–64.5°S	85–113	**	129 ± 2	8.5 ± 0.1	15.2 ± 0.3	0.70 ± 0.05	1.57 ± 0.12	82 ± 2
Geosecs	15°N–10°S	440–450	0.7b–12	129 ± 2	11.5 ± 0.2	11.2 ± 0.3	0.73 ± 0.02	1.46 ± 0.04	88 ± 2
	10°S–30°S	436–439	0.4b–12	137 ± 1	10.2 ± 0.1	13.4 ± 0.2	0.71 ± 0.01	1.52 ± 0.02	90 ± 1
	39°S–63°S	429–434	0–2.6	126 ± 2	9.0 ± 0.1	14.0 ± 0.3			

^aCharacter “b” after a number in the θ column represents the potential temperature of bottom water. Without “b” means no bottom water samples were used in the model calculation. Symbols: *, $\theta \geq (S - 34.74) \times 3.8/0.24 + 1.8$; **, $\theta \geq (S - 34.72) \times 4/0.12 + 2$ in the θ - S diagram, i.e., samples above the Circumpolar Water.

Table 1c. Remineralization Ratios Based on the WOCE and GEOSECS Sections in the Pacific Ocean^a

Section	Latitude Interval	Station Number	θ , °C	r_p ($-\text{O}_2/\text{P}$)	r_n ($-\text{O}_2/\text{N}$)	r_p/r_n (N/P)	β_3	r_c ($-\text{O}_2/\text{C}_{\text{org}}$)	r_p/r_c ($\text{C}_{\text{org}}/\text{P}$)
Redfield				138	8.6	16	0.83	1.30	106
p14N	52°N–45°N	20–34	1b–4.3	176 ± 4	13.1 ± 0.4	13.4 ± 0.5	0.76 ± 0.03	1.39 ± 0.06	127 ± 5
	45°N–26.5°N	35–72	1b–12	165 ± 3	12.0 ± 0.2	13.8 ± 0.3	0.70 ± 0.01	1.53 ± 0.03	108 ± 3
	26°N–11.5°N	73–102	0.8b–6	162 ± 4	11.6 ± 0.2	14.0 ± 0.4	0.83 ± 0.02	1.28 ± 0.03	127 ± 4
			6–12	136 ± 1	12.0 ± 0.1	11.3 ± 0.1	0.82 ± 0.01	1.29 ± 0.02	105 ± 1
	11°N–4°N	103–126	0.8b–10.5	173 ± 6	12.7 ± 0.4	13.7 ± 0.6	0.85 ± 0.03	1.24 ± 0.05	140 ± 7
p15N	54°N–41°N	2–31	1b–6	174 ± 2	12.8 ± 0.1	13.6 ± 0.2	0.71 ± 0.01	1.50 ± 0.02	116 ± 2
	40°N–26.5°N	32–59	1b–12	165 ± 4	12.5 ± 0.2	13.2 ± 0.4	0.71 ± 0.02	1.50 ± 0.05	110 ± 3
	26°N–12.5°N	66–87	0.8b–6	152 ± 6	11.7 ± 0.4	13.0 ± 0.7	0.83 ± 0.03	1.28 ± 0.05	119 ± 6
	12°N–0°	88–111	0.65b–12	170 ± 7	12.9 ± 0.4	13.2 ± 0.7	0.80 ± 0.03	1.32 ± 0.05	129 ± 7
	0°–12°S	115–136	0.65b–6	165 ± 4	12.7 ± 0.1	13.0 ± 0.3	0.80 ± 0.02	1.32 ± 0.04	125 ± 5
p15S	9.5°S–15.5°S	146–182	0.6b–2	173 ± 3	11.9 ± 0.4	14.5 ± 0.6	0.87 ± 0.05	1.21 ± 0.07	143 ± 5
			2–12	128 ± 1	8.9 ± 0.1	14.4 ± 0.2	0.68 ± 0.01	1.61 ± 0.03	79 ± 1
	16°S–42°S	89–145	0.5b–2	158 ± 4	12.0 ± 0.3	13.2 ± 0.5	0.90 ± 0.08	1.17 ± 0.11	135 ± 5
			2–10	123 ± 3	9.2 ± 0.2	13.4 ± 0.4	0.62 ± 0.03	1.78 ± 0.10	69 ± 2
	43°S–53°S	61–87	1.8–11.3	148 ± 1	9.9 ± 0.1	14.9 ± 0.2	0.59 ± 0.01	1.87 ± 0.04	79 ± 1
	53°S–64°S	36–60	–1–8 ^b	136 ± 1	9.2 ± 0.1	14.8 ± 0.2	0.62 ± 0.01	1.78 ± 0.03	76 ± 1
p14S	53°S–67°S	4–32	1.7–7.6	136 ± 4	9.3 ± 0.2	14.6 ± 0.5	0.66 ± 0.02	1.66 ± 0.06	82 ± 3
P18	16°S–28.5°S	82–107	1.5–12	123 ± 2	8.7 ± 0.2	14.1 ± 0.4	0.61 ± 0.02	1.82 ± 0.07	67 ± 2
	29°S–40.5°S	58–81	1.5–6.5	129 ± 2	10.1 ± 0.2	12.8 ± 0.3	0.63 ± 0.01	1.73 ± 0.03	74 ± 2
	54.5°S–67°S	10–33	2–7	131 ± 2	8.8 ± 0.3	14.9 ± 0.6	0.66 ± 0.03	1.67 ± 0.09	79 ± 3
Geosecs	50°N–40°N		1b–8	176 ± 1	11.6 ± 0.1	15.2 ± 0.2	0.74 ± 0.02	1.44 ± 0.04	122 ± 1
	35°N–25.5°N		0.9b–12	158 ± 2	12.1 ± 0.1	13.1 ± 0.2	0.80 ± 0.03	1.32 ± 0.05	119 ± 2
	25°N–10°N		0.8b–6	152 ± 4	11.6 ± 0.3	13.1 ± 0.5			
	9°N–13.5°S		0.6b–12	159 ± 5	11.8 ± 0.2	13.5 ± 0.5	0.83 ± 0.05	1.27 ± 0.08	125 ± 4
	15°S–42°S		2–12	152 ± 5	10.0 ± 0.2	15.2 ± 0.6			
	46.5°S–53°S		2–12	137 ± 3	9.9 ± 0.3	13.8 ± 0.5			
	54°S–69°S		2–6	148 ± 3	8.8 ± 0.3	16.8 ± 0.7	0.70 ± 0.07	1.56 ± 0.17	95 ± 4

^aCharacter “b” in the θ column represents the potential temperature of bottom water.

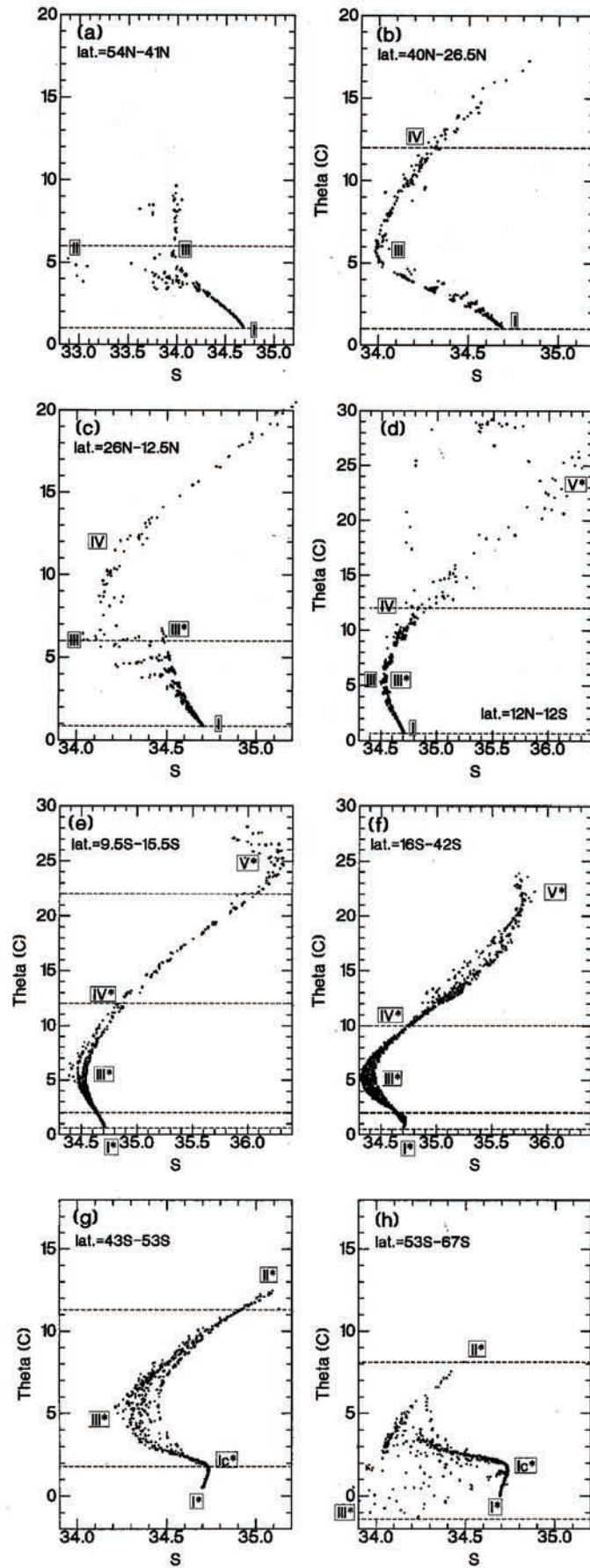
^bSamples above the Circumpolar Water.

by mixing end-members I, II, and III. Similarly, in Figure 1b, data points with θ between 1 and 12°C can be formed by the mixing of end-members I, III, and IV, and so forth. The end-members of water masses depicted in Figures 1a to 1h are as follows. I = North Pacific Bottom Water, I* = South Pacific Bottom Water, Ic* = Antarctic Circumpolar Water, II = Subarctic Water, II* = Subantarctic Water, III = North Pacific Intermediate Water, III* = Antarctic Intermediate Water, IV = North Pacific Shallow Salinity Minimum Water, IV* = South Pacific Shallow Oxygen Minimum Water, and V* = South Pacific Subtropical Salinity Maximum Water. One end-member may appear more than once in Figures 1a to 1h, but the end-member values for θ and S may not be always the same due to mixing effect of other end-members. For example, end-member III* (Antarctic Intermediate Water) appears in Figures 1d to 1h, but its θ and S values change gradually from south to north due to mixing inputs from end-members I*, Ic*, II*, and IV*. Therefore, in each chosen latitudinal interval, end-member III* has its own local end-member characteristics. Fortunately, our model requires no knowledge on end-member values of θ , S, and other variables for any chosen latitudinal interval.

[19] The data in Figure 1e are further separated into three temperature intervals, i. e., $\theta = 0.6 \sim 2.1$, $\theta = 2.1 \sim 12$, and $\theta = 12 \sim 22^\circ\text{C}$. Hydrographic data from the first two intervals are plotted in Figures 2 and 3. The obvious outliers in those plots, especially in the θ -S (Figure 2a) and PO_4 - NO_3 plots (Figures 2d and 3d), can be eliminated before regression analysis. The PO_4 - NO_3 plot is useful in testing the internal consistency of phosphate and nitrate data and in

detecting any additional new end-member with a low N/P ratio due to localized denitrification in the water column or at the nearby water-sediment interface [Broecker and Peng, 1982; Gruber and Sarmiento, 1997]. Figure 4 exemplifies the good correlation between the observed and calculated O_2 from equation (2a), and between the observed and calculated DA from equation (4c) for the data from three different temperature segments in Figure 1e. By eliminating obvious outliers in Figures 2 and 3, one can easily improve the square of the multiple correlation (R^2) up to 0.98 or higher for most cases. According to Figure 1e, the break at $\theta = 2.1^\circ\text{C}$ is not obvious. However, if one fits the data between $\theta = 0.6$ and 12°C together, there are clear breaks in the plots of the observed O_2 versus the calculated O_2 , and observed versus calculated DA as shown in Figures 4e and 4f. Those breaks correspond to θ around 2.1°C . Water with $\theta = 2.1^\circ\text{C}$ represents a local end-member probably formed by mixing the North and South Pacific Bottom Waters, Antarctic Circumpolar Water, and Antarctic Intermediate Water.

[20] The WOCE station data were obtained from the website administered by the WOCE Hydrographic Program Office (<http://whpo.ucsd.edu>). For the present study, we selected only meridional sections a17 (1994) and a20 (1997) from the western Atlantic; i8 (1994–1995) and i9 (1994–1995) from the eastern Indian Ocean; and p14 (1993 and 1996), p15 (1994 and 1996) and p18 (1994) from the central and eastern Pacific oceans. Exact locations of those sections can be found in the same website. Those selected sections provide a complete set of data on θ , S, O_2 , NO_3 , PO_4 , DIC, and Alk. When all WOCE data become publicly available, especially DIC and alkalinity



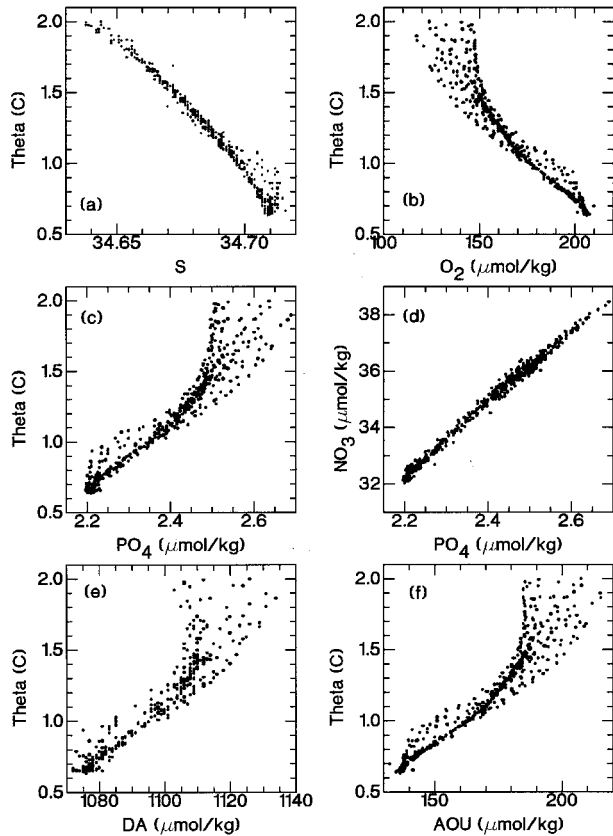


Figure 2. Various xy plots of hydrographic data from the p15 transect in latitudinal interval between 9.5°S and 15.5°S (as shown in Figure 1e) with potential temperature (θ) range between 0.6° and 2.1°C .

data, we will expand our scope of analysis. Also we present here only the results from water samples with θ below 12°C . The water samples with θ greater than 12°C often require more than three-end-member mixing and are thus beyond the present model analysis. Since θ and S are often no longer conservative in the surface oceans due to air-sea heat exchange and water evaporation/precipitation, the samples shallower than 100 m are also excluded. As will be discussed later, some bottom water samples, where the oxygen profile can be explained solely by water mass mixing (that is, the water mixing rate is much faster than the oxygen consumption rate), are also excluded from the regression analysis. Data from the northern part of the WOCE section p18 ($<15^{\circ}\text{S}$) indicate intensive denitrification both in sediments and the water column [Gruber and Sarmiento, 1997; Deutsch et al., 2001], thus they are also excluded here but will be treated in a separate paper.

[21] Some useful cross-sectional contour diagrams for the WOCE data can be found in a website at the Alfred Wegener Institute, Germany (<http://www.awi-bremerhaven.de/GEO/eWOCE/Gallery/#>). The selected GEOSECS (Geochemical Ocean Section Study) data in this paper include only station numbers between 27 and 68 from the western Atlantic Ocean (in the year 1972), between 429 and 450 from the eastern Indian Ocean (1978), and between 212 and 287 from the middle Pacific Ocean (1973–1974). Those stations are close to the WOCE stations used in this paper. The GEOSECS data can be obtained from the NOAA/AOML data management website <http://www.aoml.noaa.gov/ocd/oaces>.

3. Results and Discussion

[22] Results of multiple regression analysis from three major oceans between given latitudinal intervals and potential temperature ranges are summarized in Tables 1a, 1b, and 1c, and are plotted in Figures 5, 6, and 7 as a function of latitude. The r_p , r_n , and r_c in those tables are all averaged values (i. e. $[\tau_1 + \tau_1']/2$). Other ratios are basically calculated from r_p , r_n , and r_c . The r_c and r_p/r_c values for some GEOSECS segments are not given, because DIC and alkalinity data for those segments are too noisy to provide meaningful results. Since the chosen data all can be fitted nicely to our model, the implicit assumption of our model that remineralization ratios are constant with depth within the chosen potential temperature interval is a good one.

[23] Based on the general variation patterns of remineralization ratios shown in Figures 5, 6, and 7, the stations in the Atlantic Ocean are divided into a northern group (45°N – 5°N) and a southern group (5°N – 50°S). Similarly, the Indian Ocean stations are divided into an equatorial group (20°N – 20°S) and a southern group (30°S – 65°S), and the Pacific Ocean also into a northern group (55°N – 10°S plus bottom water mass between 10°S and 40°S) and a southern group (10°S – 70°S). The average remineralization ratios for those groups, as based only on the WOCE results in Tables 1a to 1c, are summarized in Table 2.

3.1. Atlantic Ocean

[24] Bottom water samples with θ below 2 to 3°C in the northern and below 0.2 to 0.4°C in the southern stations are not included in the regression analysis (Table 1a). As mentioned earlier, oxygen concentration profiles of those bottom samples can be explained solely by water mass mixing (no apparent in situ oxygen consumption).

[25] According to Table 1a, differences in the remineralization ratios between low and high temperature intervals are small, thus, to a first approximation, the remineralization ratios can be considered constant with depth in the Atlantic Ocean with θ below 12°C . As shown in Figures 5a, 5b, and

Figure 1. (opposite) The θ - S plots of the WOCE Pacific p15 transect data from different latitudinal intervals (north to south). Roman numerals represent various end-members of water masses in the Pacific Ocean: I = North Pacific Bottom Water, I* = South Pacific Bottom Water, Ic* = Antarctic Circumpolar Water, II = Subarctic Water, II* = Subantarctic Water, III = North Pacific Intermediate Water, III* = Antarctic Intermediate Water, IV = North Pacific Shallow Salinity Minimum Water, IV* = South Pacific Shallow Oxygen Minimum Water, and V* = South Pacific Subtropical Salinity Maximum Water.

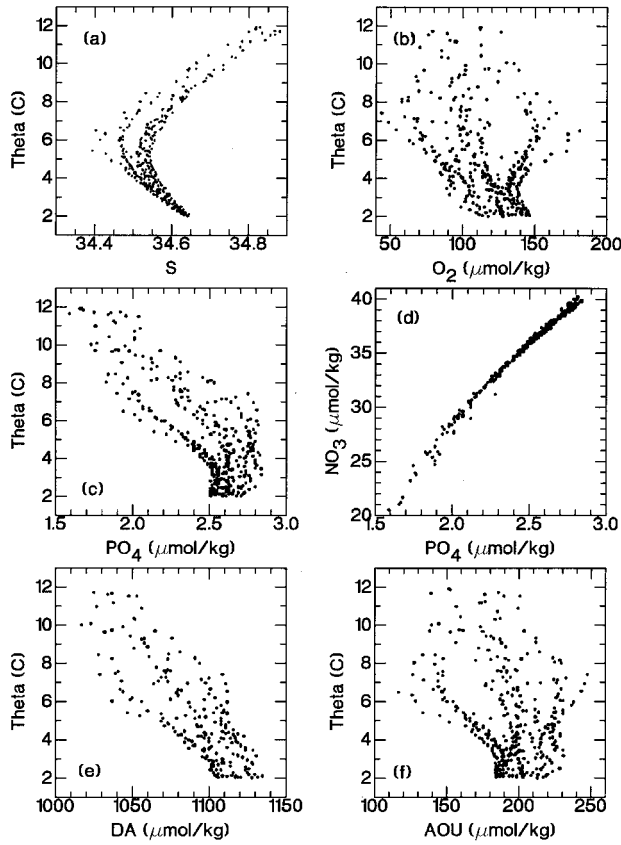


Figure 3. Same as Figure 2, except with potential temperature (θ) range between 2.1° and 12°C.

5d, the $-O_2/P$ ($= r_p$), $-O_2/N$ ($= r_n$) and N/P ($= r_p/r_n$) ratios are near constant from north to south for both WOCE and GEOSECS station data. However, the $-O_2/P$ and N/P ratios have a slight tendency to decrease from north to south for WOCE data. There are some minor disagreements in the $-O_2/P$ and N/P values between WOCE and GEOSECS data in the latitudinal interval between 0°S and 20°S. The $-O_2/P$ and N/P ratios from GEOSECS data tend to be slightly lower (Table 1a). The $-O_2/C_{org}$ ($= r_c$) ratio is near constant in the latitudinal interval between 50°S and 10°N and increases suddenly northward (Figure 5c). Since the $-O_2/N$ ratio is constant (Figure 5b), the sudden increase in the $-O_2/C_{org}$ ratio is mostly caused by decrease in organic carbon content of remineralized organic matter in the northern Atlantic Ocean. The $-O_2/C_{org}$ ratio (Figure 5c) is much higher and the C_{org}/P ratio (Figure 5e) much lower than the traditional Redfield ratios. This implies a low carbon content of remineralized organic matter in the Atlantic Ocean as compared to Redfield's average marine plankton. Interestingly, the C_{org}/P ratio is near constant from north to south (Figure 5e).

[26] The average remineralization ratios, as normalized to P, for the northern Atlantic group are $P/N/C_{org}/-O_2 = 1/(16.1 \pm 1.0)/(73 \pm 8)/(137 \pm 7)$ (Table 2). Those values are in good agreement with the traditional Redfield ratios of $P/N/C_{org}/-O_2 = 1/16/106/138$, except for the low C_{org}/P ratio. However, the uncertainties of the traditional Redfield ratios

are never given. If the traditional Redfield ratios represent the average composition of living marine plankton, then those ratios can easily have a standard deviation of more than 50% [Li *et al.*, 2000]. The model-derived remineralization ratios given here represent the average composition of remineralized nonliving organic matter (both particulate and dissolved) in the water column. The average remineralization ratios of $P/N/C_{org}/-O_2 = 1/(15.2 \pm 0.7)/(79 \pm 6)/(128 \pm 5)$ for the southern Atlantic group (Table 2) are the same as those for the northern Atlantic group within the estimated uncertainties. Average remineralization ratios for the Atlantic Ocean as obtained from WOCE and GEOSECS data sets are also the same statistically (Table 1a).

[27] Using GEOSECS data, Takahashi *et al.* [1985] obtained remineralization ratios of $P/N/C_{org}/-O_2 = 1/(16.8 \pm 1.3)/(92 \pm 12)/(178 \pm 11)$ for the Atlantic thermocline water ($\sigma_\theta = 27.20$) between a wide latitudinal interval (38°N to 45°S). Those values agree reasonably well with the present study, except that their $-O_2/P$ value is much higher than our model-derived 133 ± 5 . Broecker *et al.* [1985] and Anderson and Sarmiento [1994] also gave a high $-O_2/P$ ratio of 170 ± 10 for the whole ocean. The disagreement on the estimate of the $-O_2/P$ ratio primarily results from the

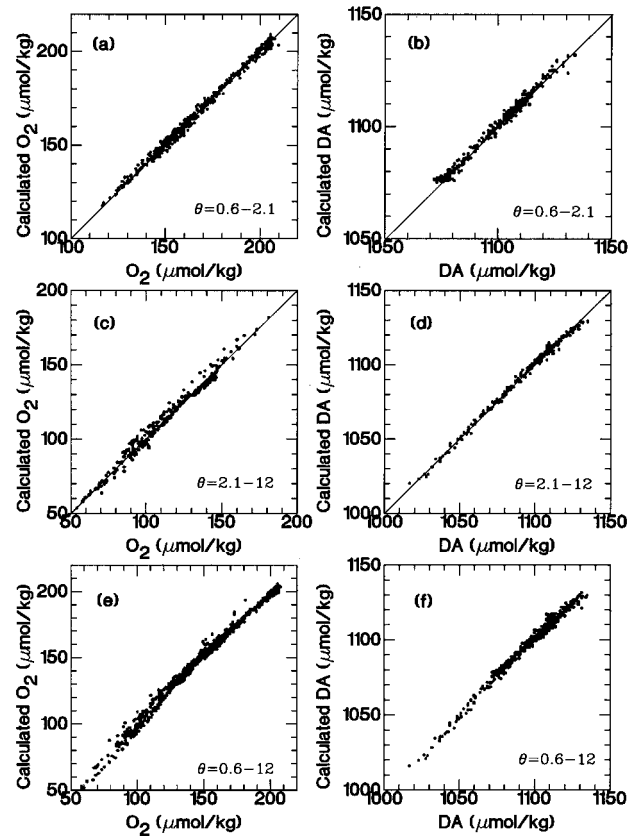


Figure 4. Comparison of the model calculated versus observed O_2 and DA for the p15 transect in latitudinal interval between 9.5°S and 15.5°S and at three different potential temperature ranges ($\theta = 0.6-2.1^\circ\text{C}$; $\theta = 2.1-12^\circ\text{C}$; and $\theta = 0.6-12^\circ\text{C}$).

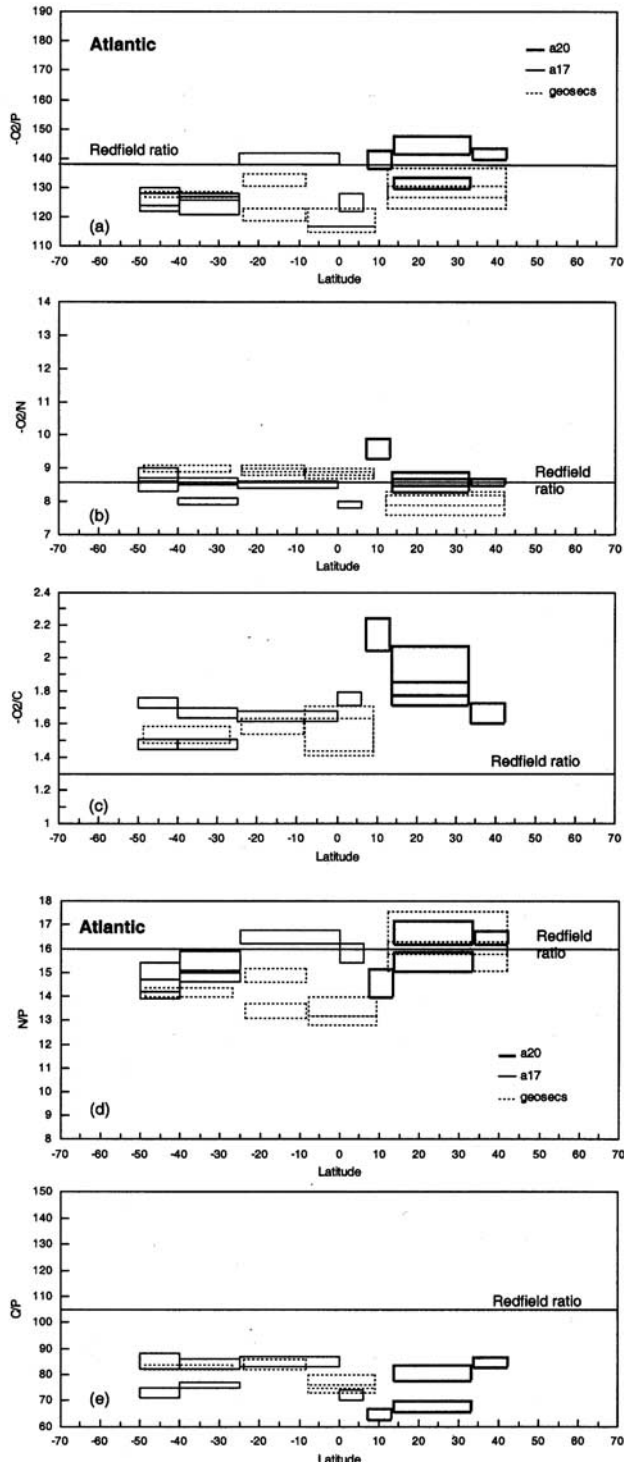


Figure 5. Various remineralization ratios as a function of latitude in the Atlantic Ocean (data from Table 1a). The solid boxes are derived from WOCE data, and dashed boxes are from GEOSECS data. The traditional Redfield Ratio is drawn in each panel for reference.

way samples were chosen for the earlier models. For example, the θ -S diagrams for the same samples used by *Takahashi et al.* [1985] in their two-end-member mixing model show a distinct break in slopes (Figures 8a and 8b),

indicating mixing of at least three end-members. Therefore, they should not have used all those samples, which cover a wide latitudinal range, in their two-end-member mixing model. When their northern Atlantic data alone were fitted

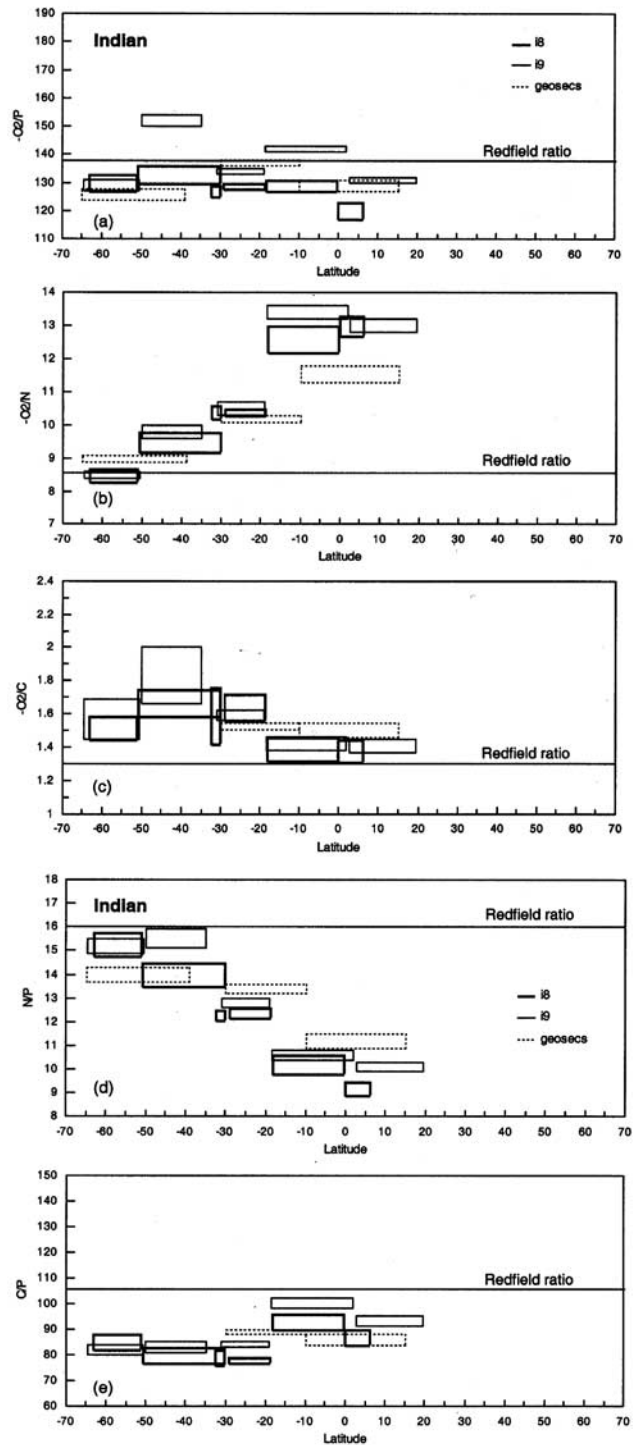


Figure 6. Various remineralization ratios as a function of latitude in the Indian Ocean (data from Table 1b). The solid boxes are derived from WOCE data, and dashed boxes are from GEOSECS data. The traditional Redfield Ratio is drawn in each panel for reference.

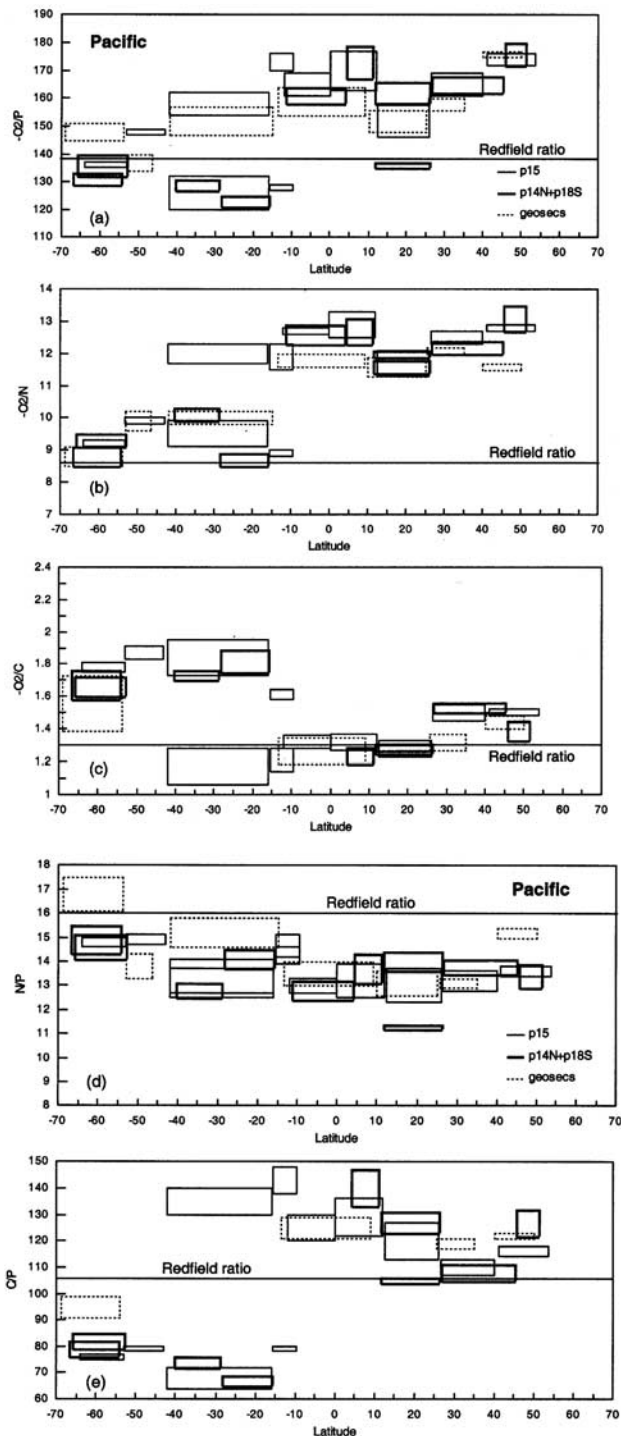


Figure 7. Various remineralization ratios as a function of latitude in the Pacific Ocean (data from Table 1c). The solid boxes are derived from WOCE data, and dashed boxes are from GEOSECS data. The traditional Redfield Ratio is drawn in each panel for reference.

to the two-end-member mixing model of *Li et al.* [2000], an $-O_2/P$ ratio of 140 ± 10 was obtained, in good agreement with the present result. *Anderson and Sarmiento* [1994] put together neutral surface data from a wide latitudinal interval ($20^\circ N$ to $50^\circ S$) for the South Atlantic Ocean. *Peng and Broecker* [1987] also treated together isopycnal horizon data (with $\theta = 1.4 \pm 0.1^\circ C$; depth about 3000 m) from a wide latitudinal interval ($45^\circ N$ to $43^\circ S$) in the Pacific Ocean. The θ -S plot of samples used by *Peng and Broecker* [1987] appears to suggest a two-end-member mixing at first glance (Figure 8c), but diapycnal mixing inputs of other water masses is unavoidable over such a wide latitudinal interval. Indeed, an irregular O_2 distribution pattern in the θ - O_2 plot of their original data (Figure 8d) suggests mixing of at least three to four end-members. As shown in Figures 1a to 1g, the water mass with $\theta = 1.4 \pm 0.1^\circ C$ is formed not only by mixing North Pacific Bottom Water (I) and South Pacific Bottom Water (I*), but also Antarctic Circumpolar Water (I*), Antarctic Intermediate Water (III*), and North Pacific Intermediate Water (III). One may avoid the problem by choosing data from a narrower latitudinal interval, but very often the number of available data points becomes rather small for any horizontal two-end-member mixing model.

[28] An additional problem with earlier models was the way the end-member values were assigned. For example, *Takahashi et al.* [1985] plotted θ versus O_2 data from an isopycnal horizon and extrapolated linearly the correlation line to intercept with the oxygen solubility line in equilibrium with the atmosphere (as a function of θ). The values of θ and O_2 at the intercept were adapted as the end-member values. However, O_2 is a nonconservative tracer; thus there is no a priori reason to believe a plot of θ versus O_2 should be always linear. If it is really linear, then there is no oxidation of organic matter. *Broecker et al.* [1985] plotted PO_4 versus O_2 from an isopycnal horizon to obtain the slope of $-O_2/P (= r_p)$. Their implicit assumption was that the concentrations of PO_4 and O_2 for the two mixing end-members are identical or similar, which is not always a good assumption. *Broecker et al.* [1985] also plotted $(PO_4 - PO_4^0)$ versus $(O_2 - O_2^0) (= AOU)$ to obtain the $-O_2/P$ ratio. However, the procedure for assigning values of preformed phosphate (PO_4^0) is problematic, as was also the case for *Takahashi et al.* [1985].

[29] The average composition of sediment trap materials obtained at the Ocean Flux Program (OFP)/ Bermuda Atlantic Time Series (BATS) site is $P/N/C_{org} = 1/(20 \pm 7)/(180 \pm 70)$ over a depth range between 500 and 3200 m [*Conte et al.*, 2001]. Therefore, the composition of remineralized organic matter in the water column is quite different from that of sediment trap materials. Sediment trap materials must be mostly leftover materials after remineralization and may have preferentially lost P over N (N/P ratio of 20 versus 15), and N over C_{org} (C_{org}/N ratio of 9 ± 4.7 versus 4.6 ± 0.6) as compared to the remineralized organic matter. The C_{org}/N ratio for the total organic matter (dissolved and particulate) at BATS site at a depth interval between 1000 and 4000 m is 14.1 ± 1.8 [*Hansell and Carlson*, 2001]. This ratio is again much larger than those of marine plankton ($C_{org}/N = 6.6$) and remineralized organic matter ($C_{org}/N =$

Table 2. Average Remineralization Ratios of Organic Matter in Three Major Oceans (Based Only on WOCE Data)^a

	Latitude Interval	P/P	N/P (r_p/r_n)	C_{org}/P (r_p/r_c)	$-O_2/P$ (r_p)	$-O_2/N$ (r_n)	$-O_2/C_{org}$ (r_c)	C_{org}/N (r_n/r_c)
Redfield		1	16	106	138	8.6	1.30	6.6
				<i>Atlantic</i>				
North	45°N–5°N	1	16.1 ± 1.0	73 ± 8	137 ± 7	8.5 ± 0.8	1.9 ± 0.2	4.6 ± 0.6
South	5°N–50°S	1	15.2 ± 0.7	79 ± 6	128 ± 5	8.4 ± 0.3	1.6 ± 0.1	5.2 ± 0.4
				<i>Indian</i>				
Equator	20°N–20°S	1	10.3 ± 0.7	94 ± 5	130 ± 7	12.7 ± 0.7	1.4 ± 0.1	9.2 ± 0.5
			(15 ± 1)	(92 ± 5)	130 ± 7	(8.7 ± 0.6)	(1.4 ± 0.1)	(6.1 ± 0.5)
South	30°S–65°S	1	14.8 ± 0.7	83 ± 2	134 ± 9	9.1 ± 0.8	1.6 ± 0.1	5.6 ± 0.6
				<i>Pacific</i>				
North	55°N–10°S ^b	1	13.3 ± 0.9	124 ± 11	162 ± 11	12.2 ± 0.5	1.3 ± 0.1	9.2 ± 0.8
			(15 ± 1)	(123 ± 11)	162 ± 11	(10.8 ± 0.7)	(1.3 ± 0.1)	(8.2 ± 0.8)
South	10°S–70°S	1	14.5 ± 1.0	78 ± 7	136 ± 10	9.4 ± 0.5	1.7 ± 0.1	5.4 ± 0.4
				<i>Other</i>				
Southern Oceans ^c		1	15 ± 1	80 ± 3	133 ± 5	9.0 ± 0.4	1.6 ± 0.1	5.4 ± 0.3

^aValues in parenthesis are obtained by assuming $r_n = r_p/15$, i.e. $N/P = 15$.

^bPlus bottom water mass between 10°S and 40°S.

^cAverage of the south from three oceans.

4.6 ± 0.6) in the water column, again suggesting preferential loss of N.

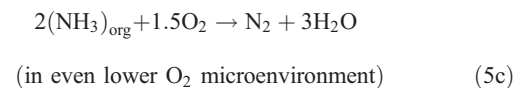
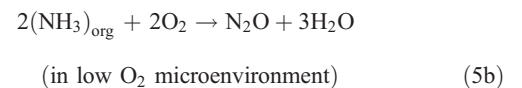
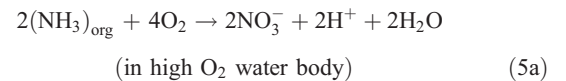
3.2. Indian Ocean

[30] The O_2 data for the bottom water samples with θ less than 2°C in the southern Indian Ocean show no apparent in situ oxygen consumption and can be explained by water mass mixing, thus are again excluded (Table 2b). Remineralization ratios given in Figures 6a to 6e for the southernmost stations of the Indian Ocean are all similar to those for the southernmost stations of the Atlantic Ocean. The $-O_2/P$ ratio is nearly constant (close to the traditional Redfield ratio; Figure 6a), but the $-O_2/N$ ratio increases steadily from the southern (close to the traditional Redfield ratio) to equatorial Indian oceans (Figure 6b). This may indicate a steady decrease of net nitrate input relative to both P input and oxygen consumption during oxidation of organic matter in the water column. The steady decrease of the N/P ratio from the south (close to the traditional Redfield ratio) to the equator (Figure 6d) is consistent with this explanation. The $-O_2/C_{org}$ (Figure 6c) and P/C_{org} (inverse of Figure 6e) ratios decrease slightly from the south to the equator, while the $-O_2/P$ ratio is nearly constant (Figure 6a). These observations suggest that C_{org} input increases slightly relative to both P input and oxygen consumption from the south to the equator during oxidation of organic matter in the Indian Ocean.

[31] The average remineralization ratios of $P/N/C_{org}/-O_2 = 1/(14.8 \pm 0.7)/(83 \pm 2)/(134 \pm 9)$ for the southern Indian group (30°S–65°S) are statistically identical to those for the southern Atlantic group (Table 2). In contrast, average remineralization ratios for the equatorial Indian group are $P/N/C_{org}/-O_2 = 1/(10.3 \pm 0.7)/(94 \pm 5)/(130 \pm 7)$. The low N/P ratio here may indicate either a truly low N/P ratio in the remineralized organic matter, or more likely the loss of nitrate during the oxidation process of organic matter throughout the water column. If the actual mineralization ratio of N/P ($= r_p/r_n$) is 15 ± 1 (or $r_n = r_p/15 = 8.7 \pm 0.6$) for remineralized organic matter in the equatorial Indian Ocean, then the model

derived N/P ratio of 10 ± 1 may suggest the following. One third ($= (15-10)/15$) of organic nitrogen converts into gaseous N_2 and N_2O instead of usual NO_3^- during oxidation process of organic matter. Therefore, the true average remineralization ratios of organic matter in the equatorial Indian Ocean could be $P/N/C_{org}/-O_2 = 1/(15 \pm 1)/(92 \pm 5)/(130 \pm 7)$ (Table 2, parenthesis), which are similar to those for the southern Atlantic and Indian oceans, except slightly higher C_{org}/P ratio (Table 2). The fraction of organic nitrogen converted into N_2 and N_2O must have been fairly constant throughout the water column. If the conversion were uneven and localized, one would not expect to obtain the observed good model fit. In order to calculate the preformed nitrate ($= NO_3^- - AOU/r_n$), one still needs to use the model-derived r_n of 12.7 ± 0.7 to account for a partial conversion of organic nitrogen into N_2 and N_2O . Notice here that the change of the r_n value from 12.7 to 8.7 would increase only slightly the r_c value from 1.39 to 1.42, and the r_p/r_c ratio from 94 to 92.

[32] One may postulate that the partial conversion of organic nitrogen, as $(NH_3)_{org}$, into N_2 and N_2O is facilitated by bacteria within a low-oxygen microenvironment of organic matter during the nitrification process of organic nitrogen. For example, overall net reactions could be:



The traditional thinking is that all organic nitrogen is first converted into $NO_2^- + NO_3^-$ during water column nitrification process [von Brand *et al.*, 1937]. Then, some fraction of NO_2^-

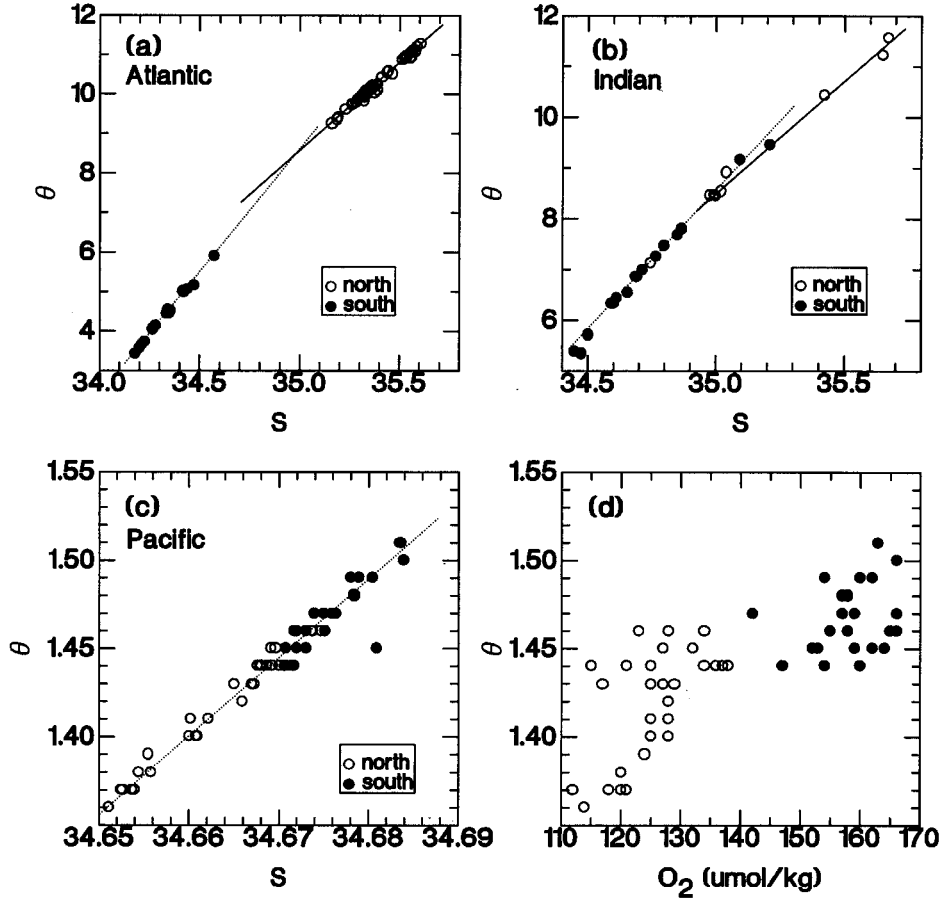
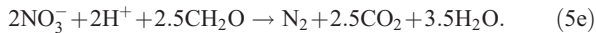
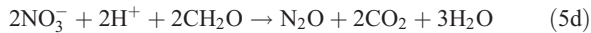


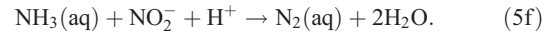
Figure 8. Plots of salinity (S) versus potential temperature (θ) data from (a) the Atlantic thermocline water along the $\sigma_{\theta} = 27.2$ horizon [Takahashi *et al.*, 1985], (b) the Indian thermocline water along $\sigma_{\theta} = 27.2$ horizon [Takahashi *et al.*, 1985], and (c) the deep Pacific Ocean along the $\sigma_4 = 45.83$ per mil isopycnal horizon [Peng and Broecker, 1987]. (d) Plot of dissolved oxygen (O_2) versus θ along the $\sigma_4 = 45.83$ per mil isopycnal horizon in the deep Pacific Ocean [Peng and Broecker, 1987].

+ NO_3^- is reduced back to gaseous N_2O and N_2 during denitrification process within a reducing microenvironment of organic matter by bacteria. For example:



The low oxygen or reducing microenvironment is a necessary condition here, because all the water samples selected for our model calculations have moderate to high oxygen concentrations. Production of N_2O and N_2 gaseous species during the denitrification process is well documented [Karl and Michaels, 2001, and references therein; Naqvi *et al.*, 2000]. Production of N_2O during the nitrification process has also been demonstrated [Yoshinari, 1976; Elkins *et al.*, 1978; Goreau, 1980]. Unfortunately none of them specifically looked for N_2 . It will be interesting to design experiments to test the formation of N_2 during the nitrification process of organic nitrogen. It has been shown recently [Strous *et al.*, 1999] that planctomycete bacteria

can produce N_2 by the anammox (anaerobic ammonia oxidation) reaction:



The lesson is that we are still quite ignorant about many novel metabolic pathways of nitrogen by bacteria in natural environments [Amend and Shock, 2001].

[33] Peng and Broecker [1987] gave average remineralization ratios of $P/N/C_{org}/-O_2 = 1/(13.4 \pm 1.0)/(135 \pm 18)/(176 \pm 11)$ for the deep Indian Ocean. Takahashi *et al.* [1985] gave $P/N/C_{org}/-O_2 = 1/(14.5 \pm 0.5)/(125 \pm 7)/(174 \pm 6)$ for the Indian thermocline water. These values are quite different from the present study. Their C_{org}/P and $-O_2/P$ ratios are especially high. Possible causes for their high ratios were already discussed in the last section.

3.3. Pacific Ocean

[34] Bottom water samples with θ less than 1.5 to 2°C in the southern Pacific Ocean (latitude $>40^\circ S$; Table 1c) are excluded again, because the oxygen profiles there can be

explained solely by water mass mixing. The northern Pacific group (55°N to 10°S plus the bottom water mass between 10°S and 40°S) is characterized by constantly high $-O_2/P$ and $-O_2/N$, and low N/P ratios (Figures 7a, 7b, and 7d), as compared to the traditional Redfield ratios and to those for the southern Pacific group. The implication is that oxygen consumption is high in the northern Pacific group and there is a moderate but significant conversion of organic nitrogen into N_2 and N_2O through nitrification/denitrification reactions, as seen for the equatorial Indian group. The constantly low $-O_2/C_{org}$ (Figure 7c) and P/C_{org} ratios (inverse of Figure 7e), as compared with the southern Pacific group, also suggest a high carbon content of remineralized organic matter in the water column of the northern Pacific group.

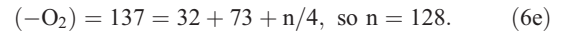
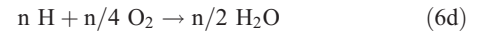
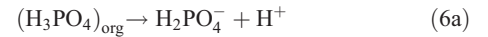
[35] As shown in Table 2, the average remineralization ratios of $P/N/C_{org}/-O_2 = 1/(14.5 \pm 1.0)/(78 \pm 7)/(136 \pm 10)$ for the southern Pacific group are essentially the same as those for the southern Atlantic and the southern Indian oceans within the estimated uncertainties. We may classify them together as the Southern Oceans group, having average remineralization ratios of $P/N/C_{org}/-O_2 = 1/(15 \pm 1)/(80 \pm 3)/(133 \pm 5)$ (Table 2). The average remineralization ratios of $P/N/C_{org}/-O_2 = 1/(13.3 \pm 0.9)/(124 \pm 11)/(162 \pm 11)$ for the northern Pacific group are in good agreement with $P/N/C_{org}/-O_2 = 1/(13 \pm 1)/(135 \pm 18)/(170 \pm 9)$ for the ALOHA station in the subtropical North Pacific [Li *et al.*, 2000]. Peng and Broecker [1987] gave $P/N/C_{org}/-O_2 = 1/(14.8 \pm 1)/(130 \pm 16)/(199 \pm 10)$ for the deep Pacific Ocean, which is also similar to the present estimate for the northern Pacific group, except for their high $-O_2/P$ ratio. The low N/P ratio of 13 ± 1 in the northern Pacific group may represent either a true low N/P ratio in remineralized organic matter or most likely the conversion of some organic nitrogen into N_2O and N_2 during the nitrification/denitrification processes, as is the case for the equatorial Indian group. The actual N/P ratio for the remineralized organic matter could also be around 15 ± 1 (or $r_n = r_p/15 = 10.8 \pm 0.7$). As discussed in the Indian Ocean section, the fraction of organic nitrogen converted into N_2 and N_2O must have been fairly constant throughout the water column. If not, one would not expect to have a tight correlation between PO_4 and NO_3^- concentration data, as shown in Figure 2d, and obtain the observed good model fit. To calculate the preformed nitrate one still should use the model-derived r_n value of 12.2 ± 0.5 to account for the partial conversion of organic nitrogen into N_2O and N_2 . The unusually high C_{org}/P ratio of 124 ± 11 (Table 2) for the northern Pacific group indicates high carbon content of organic matter as compared with other groups.

[36] The shallow sediment trap materials obtained at ALOHA station have an average composition of $P/N/C_{org} = 1/24/187$ at a depth of 100 m, and $P/N/C_{org} = 1/29/303$ at a depth of 500 m [Karl *et al.*, 1996, 2001a]. Those ratios suggest the preferential loss of P over N over C_{org} during shallow remineralization as compared to both plankton and remineralized organic matter, as already discussed in the Atlantic Ocean. The suspended particles collected at depths between 500 and 1000 m have an average composition of $P/N/C_{org} = 1/20/155$ [Hebel and Karl, 2001]. Furthermore,

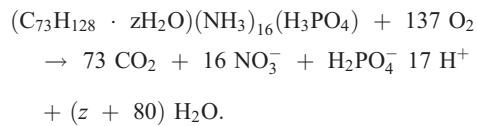
Benner [2002] gave an average composition of $P/N/C_{org} = 1/22/300$ for dissolved organic matter (DOM) from surface oceans and of $P/N/C_{org} = 1/25/444$ for DOM from deep oceans worldwide. Therefore, the composition of remineralized organic matter in the water column is again quite different from those of sediment trap materials, suspended particles, and DOM. Additional study is needed on the genetic relationship and mass balances among remineralized organic matter and other organic species such as plankton, sediment trap materials, suspended particles and DOM in a given water column.

4. Overall Discussion

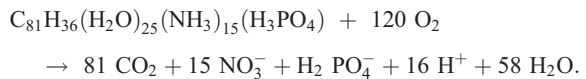
[37] One may formulate the chemical composition of one mole of a model organic matter in a water column from the average remineralization ratios ($P/N/C_{org}/-O_2$). The assumptions are as follows: phosphorus exists as H_3PO_4 , nitrogen as NH_3 , and organic carbon as a mixture of hydrocarbon and variable water ($C_mH_n \cdot zH_2O$) in the model organic matter. Oxidation of organic matter from the northern Atlantic Ocean with $P/N/C_{org}/-O_2 = 1/16/73/137$ gives the following:



By adding equations 6a through 6d, one obtains the oxidation reaction of the model organic matter, i.e.,



Similar calculations for the Southern Oceans, equatorial Indian, and northern Pacific groups are summarized in Table 3. For the equatorial Indian and northern Pacific oceans, one should also include equation 5c to take care of the partial conversion of $(NH_3)_{org}$ into N_2 (including N_2O). For comparison, one may rewrite the average composition of three mixed plankton samples from the southern Pacific Ocean ($C_{81}H_{134}O_{29}N_{15}P$; assuming N/P ratio of 15 and normalized to P) by Hedges *et al.* [2002] to $C_{81}H_{36}(H_2O)_{25}(NH_3)_{15}(H_3PO_4)$. Its oxidation gives



Therefore, one obtains the remineralization ratios of $P/N/C_{org}/-O_2 = 1/15/81/120$ for the mixed plankton, which is

Table 3. Model Compositions of 1 Mole of Remineralized Organic Matter in Different Ocean Basins^a

Ocean Basin	P/N/C _{org} /-O ₂	Model Organic Matter	-O ₂ /C _{org}	H/C	H ⁺	N ₂
Northern Atlantic	1/16/73/137	C ₇₃ H ₁₂₈ (zH ₂ O)(NH ₃) ₁₆ (H ₃ PO ₄) ^b	1.8 ^c	1.75	17	0
Southern Oceans	1/15/80/133	C ₈₀ H ₉₂ (zH ₂ O)(NH ₃) ₁₅ (H ₃ PO ₄)	1.6	1.15	16	0
Equatorial Indian	1/15/92/130	C ₉₂ H ₅₇ (zH ₂ O)(NH ₃) ₁₅ (H ₃ PO ₄)	1.4	0.62	11	2.5
Northern Pacific	1/15/123/162	C ₁₂₃ H ₄₆ (zH ₂ O)(NH ₃) ₁₅ (H ₃ PO ₄)	1.3	0.37	14	1
Redfield	1/16/106/138	C ₁₀₆ (106H ₂ O)(NH ₃) ₁₆ (H ₃ PO ₄)	1.3	0	17	0

^aCalculated from remineralization ratios (P/N/C_{org}/-O₂). H/C is the ratio of hydrogen and carbon in hydrocarbon fraction of the model organic matter. H⁺ and N₂ are the moles of produced hydrogen ion and nitrogen during oxidation of 1 mole of the model organic matter.

^bThe z in the model organic matter is unknown number of water molecules.

^cExcluded one high value at 13°N–7°N in Table 1a.

similar to that for the remineralized organic matter in the Southern Oceans (Table 2) except that -O₂/P ratio is lower. *Anderson* [1995] proposed an average formula of C₁₀₆H₄₈(H₂O)₃₈(NH₃)₁₆(H₃PO₄) for marine phytoplankton with P/N/C_{org}/-O₂ = 1/16/106/150, which is similar to the traditional Redfield ratios except the -O₂/P ratio is higher.

[38] The -O₂/C_{org} and H/C ratios of hydrocarbon fraction in the model organic matter (Table 3) decrease systematically from the northern Atlantic Ocean to the Southern Oceans, then to the equatorial Indian Ocean and the northern Pacific Ocean. The implication is that the relative proportions of biomolecules, such as lipids, proteins, nucleic acids, and carbohydrate (polysaccharides), in remineralized organic matter change systematically from ocean to ocean. According to the calculation by *Laws* [1991], the average molar ratio of production (or consumption) rate of O₂ and photosynthesis (or respiration) rate of C_{org} (-O₂/C_{org}) is about 1.6 ± 0.3 for proteins and nucleic acids, 1.4 ± 0.1 for lipids, and 1.0 ± 0.1 for polysaccharides (carbohydrate). His assumption is that organic carbon and organic nitrogen in those biomolecules are all converted from (or oxidized to) CO₂ and nitrate. *Hedges et al.* [2002] gave an average formula of C₁₀₆H₁₄(H₂O)₃₄(NH₃)₂₈(H₂S) for protein, C₁₈H₃₀(H₂O)₂ for lipid, and C₆(H₂O)₅ for carbohydrate in mixed plankton samples. Oxidation of those biomolecules gives the -O₂/C_{org} ratio of 1.63, 1.42, and 1, respectively. These values are in good agreement with *Laws*' general estimations. Therefore, the relatively high -O₂/C_{org} ratio of 1.8 to 1.6 in the northern Atlantic Ocean and the Southern Oceans (Table 2) may indicate relatively high protein and nucleic acid contents for remineralized organic matter in the water column there. The relatively low -O₂/C_{org} ratio of 1.3 to 1.4 in the equatorial Indian and the northern Pacific oceans may suggest relatively high carbohydrate and lipid contents of remineralized organic matter in those regions. Indeed, *Hedges et al.* [2002] showed that the model-derived protein content is higher, and carbohydrate and lipid are lower in the mixed plankton samples from the Southern Oceans than from the equatorial Pacific (belongs to the northern Pacific group in our classification) and the Arabian Sea.

[39] Systematic change in the biochemical compositions of both remineralized organic matter and mixed living plankton may reflect the difference in plankton populations in different oceans. For example, prokaryotic picoplankton

(*Prochlorococcus* and *Synechococcus*), eukaryotic nanoplankton, coccolithophores and pennate diatoms are dominant species in the Sargasso Sea of the North Atlantic Ocean [*DuRand et al.*, 2001]. The centric and pennate diatoms are the major phytoplankton species in the Southern Oceans [*Brown and Landry*, 2001]. In contrast, prokaryotic picoplankton (*Prochlorococcus* and *Synechococcus*) and eukaryotic picoplankton dominate in the equatorial Pacific [*Chavez et al.*, 1996; *S. Brown et al.*, Microbial absorption and backscattering coefficients from in situ and satellite data during an ENSO cold phase in the equatorial Pacific (108°), submitted to *Journal of Geophysical Research*, 2002] and in the Arabian Sea (except during southwest monsoon, diatoms become dominant) [*Garrison et al.*, 2000]. *Prochlorococcus* is the major phytoplankton taxon in the North Pacific Subtropical Gyre [*Karl et al.*, 2001b]. Certainly further study is needed.

[40] We have shown that there is a systematic change in the average remineralization ratios (P/N/C_{org}/-O₂) of remineralized organic matter from the northern Atlantic Ocean [1/(16.1 ± 1)/(73 ± 8)/(137 ± 7)] to the Southern Oceans [1/(15 ± 1)/(80 ± 3)/(133 ± 5)], then to the equatorial Indian Ocean [1/(15 ± 1)/(92 ± 5)/(130 ± 7)] and the northern Pacific Ocean [1/(15 ± 1)/(123 ± 11)/(162 ± 11)], more or less along the global deep ocean circulation route. As discussed earlier, the N/P ratio of 15 ± 1 is adopted here for the equatorial Indian Ocean and the northern Pacific Ocean to correct for the effect of nitrification/denitrification on the model-derived r_n. In contrast, *Anderson and Sarmiento* [1994] gave P/N/C_{org}/-O₂ = 1/(16 ± 1)/(117 ± 14)/(170 ± 10) for three major oceans at depths below 400 m. *Shaffer et al.* [1999] also concurred with those estimates for the major three oceans (at depth below 1500 m). However, each model has its own assumptions, and thus its own weakness and limitation. For example, the assumption by *Anderson and Sarmiento* [1994] that ΔC_{inorg}/ΔP is constant along a neutral surface is not justified by any observation. Furthermore, their neutral surfaces cover wide latitudinal intervals, thus their two-end-member mixing model ignored the effect of possible diapycnal mixing inputs from other water masses, as mentioned earlier. *Shaffer et al.* [1999] allowed some variability for initial values of end-members. However, the choice of initial values is still subjective. In our model, the preformed DA (= DIC⁰ - Alk⁰/2) is not strictly conservative in the shallow waters due to input of anthropogenic CO₂. No matter which model we use, it seems to be reasonable to

apply the remineralization ratio of $N/P = 16 \pm 1$ to the whole ocean for estimating the extent of nitrogen fixation and conversion of N_{org} into N_2 and N_2O [Gruber and Sarmiento, 1997; Deutsch et al., 2001].

[41] With a few exceptions, the remineralization ratios obtained using WOCE and GEOSECS data sets are the same within estimated uncertainties (Figures 5 to 7). The claim that the remineralization ratios in the deep oceans change with time [Pahlow and Riebesell, 2000] is premature as has been discussed by Zhang et al. [2000].

5. Summary and Conclusions

1. A new three-end-member mixing model has been introduced and successfully applied to GEOSECS and WOCE data sets to estimate remineralization ratios of organic matter (dissolved and particulate) in the water column.

2. Remineralization ratios ($P/N/C_{org}/-O_2$) of organic matter change systematically from the northern Atlantic to the Southern Oceans, then to the equatorial Indian and northern Pacific oceans, almost along the global deep ocean circulation route.

3. The average remineralization ratios of $P/N/C_{org}/-O_2$ for the northern Atlantic and the Southern Oceans groups are the same within the estimated uncertainties. The average is $P/N/C_{org}/-O_2 = 1/(15 \pm 1)/(78 \pm 8)/(134 \pm 10)$, which is similar to the traditional Redfield ratios of $P/N/C_{org}/-O_2 = 1/16/106/138$, except for the low C_{org}/P ratio. This may imply that the average compositions of remineralized organic matter and mixed marine plankton are not much different.

4. If the N/P ratio of 15 ± 1 (or $r_n = r_p/15 = 8.7 \pm 0.7$) is adopted for the equatorial Indian Ocean, the remineralization ratios there become $P/N/C_{org}/-O_2 = 1/(15 \pm 1)/(92 \pm 5)/(130 \pm 7)$, which are similar to those for the northern Atlantic and the Southern Oceans groups, except for a slightly higher C_{org}/P ratio. In order to calculate the preformed nitrate, one still needs to use the model-derived r_n value of 12.7 ± 0.7 .

5. The equatorial Indian and the northern Pacific groups are characterized by the high model-derived r_n ($= -O_2/N$) and low N/P ($= r_p/r_n$) values (Table 2). The high r_n and low N/P ratio are most likely caused by partial conversion of organic nitrogen into gaseous N_2O and N_2 throughout the water column during the nitrification/denitrification process within reducing microenvironments of organic matter by bacteria.

6. The northern Pacific group ($55^\circ N-10^\circ S$ plus bottom water mass between $10^\circ S$ and $40^\circ S$) is further characterized by the high C_{org}/P ratio (124 ± 11) as compared to other groups (83 ± 10 ; Table 2), indicating a high carbon content of remineralized organic matter.

7. The $-O_2/C_{org}$ ratio of remineralized organic matter decreases from the northern Atlantic (1.8) to the Southern Oceans (1.6), then to the equatorial Indian (1.4) and the northern Pacific (1.3) oceans. This systematic change may indicate a decreasing trend of protein plus nucleic acid and an increasing trend of carbohydrate (polysaccharide) and lipid contents in remineralized organic matter as well as mixed plankton.

8. No obvious temporal trends are detected from the remineralization ratios obtained from the GEOSECS and WOCE data sets.

[42] **Acknowledgments.** Discussions with Bob Bidigare, Susan Brown, Paul Falkowski, David Karl, and Edward Laws are most fruitful. Detailed comments by James Murray as a reviewer have greatly improved this paper. Editorial assistant from Diane Henderson is indispensable. This work is supported by the NOAA/OAR/OGP grant GC99-032. SOEST contribution 6038.

References

- Amend, J. P., and E. L. Shock, Energetics of overall metabolic reactions of thermophilic and hyperthermophilic archaea and bacteria, *FEMS Microbiol. Rev.*, 25, 175–243, 2001.
- Anderson, L. A., On the hydrogen and oxygen content of marine phytoplankton, *Deep Sea Res., Part I*, 42, 1675–1680, 1995.
- Anderson, L. A., and J. L. Sarmiento, Redfield ratios of remineralization determined by nutrient data analysis, *Global Biogeochem. Cycles*, 8, 65–80, 1994.
- Benner, R., Chemical composition and reactivity, in *Biogeochemistry of Marine Dissolved Organic Matter*, edited by D. A. Hansell and C. A. Carlson, pp. 59–90, Academic, San Diego, Calif., 2002.
- Boulaudid, M., and J. F. Minster, Oxygen consumption and nutrient regeneration ratios along isopycnal horizons in the Pacific Ocean, *Mar. Chem.*, 26, 133–153, 1989.
- Broecker, W. S., NO: A conservative water-mass tracer, *Earth Planet. Sci. Lett.*, 23, 100–107, 1974.
- Broecker, W. S., and T. H. Peng, *Tracers in the Sea*, Lamont-Doherty Earth Obs., Palisades, N. Y., 1982.
- Broecker, W. S., T. Takahashi, and T. Takahashi, Sources and flow patterns of deep-ocean water as deduced from potential temperature, salinity, and initial phosphate concentration, *J. Geophys. Res.*, 90, 6925–6939, 1985.
- Brown, S. L., and M. R. Landry, Microbial community structure and biomass in surface waters during a Polar Front summer bloom along $170^\circ W$, *Deep Sea Res., Part II*, 48, 4039–4058, 2001.
- Chavez, F. P., K. R. Buck, S. K. Service, J. Newton, and R. T. Barber, Phytoplankton variability in the central and eastern tropical Pacific, *Deep Sea Res., Part II*, 43, 835–870, 1996.
- Chen, C. T. A., and R. M. Pytkowicz, On the total CO_2 -titration alkalinity-oxygen system in the Pacific Ocean, *Nature*, 281, 362–365, 1979.
- Conte, M. H., N. Ralph, and E. H. Ross, Seasonal and interannual variability in deep ocean particle fluxes at the Ocean Flux Program (OFP)/Bermuda Atlantic Time Series (BATS) site in the western Sargasso Sea near Bermuda, *Deep Sea Res., Part II*, 48, 1471–1505, 2001.
- Deutsch, C., N. Gruber, R. M. Key, J. L. Sarmiento, and A. Ganachaud, Denitrification and N_2 fixation in the Pacific Ocean, *Global Biogeochem. Cycles*, 15, 483–506, 2001.
- DuRand, M. D., R. J. Olson, and S. W. Chisholm, Phytoplankton population dynamics at the Bermuda Atlantic Time-series station in the Sargasso Sea, *Deep Sea Res., Part II*, 48, 1983–2003, 2001.
- Elkins, J. W., S. C. Wofsy, M. B. McElroy, C. E. Kolb, and W. A. Kaplan, An aquatic sources and sinks for nitrous oxide, *Nature*, 275, 602–606, 1978.
- Garrison, D. L., et al., Microbial food web structure in the Arabian Sea: A US JGOFS study, *Deep Sea Res., Part II*, 47, 1387–1422, 2000.
- Goreau, T. J., Production of NO_2^- and N_2O by nitrifying bacteria at reduced concentrations of oxygen, *Appl. Environ. Microbiol.*, 40, 526–532, 1980.
- Gruber, N., and J. L. Sarmiento, Global patterns of marine nitrogen fixation and denitrification, *Global Biogeochem. Cycles*, 11, 235–266, 1997.
- Hansell, D., and C. A. Carlson, Biogeochemistry of total organic carbon and nitrogen in the Sargasso Sea: control by convective overturn, *Deep Sea Res., Part II*, 48, 1649–1667, 2001.
- Hebel, D., and D. M. Karl, Seasonal, interannual and decadal variations in particulate matter concentrations and composition in the subtropical North Pacific Ocean, *Deep Sea Res., Part II*, 48, 1669–1695, 2001.
- Hedges, K. I., J. A. Baldock, Y. Gelina, C. Lee, M. L. Peterson, and S. G. Wakeham, The biochemical and elemental compositions of marine plankton: A NMR perspective, *Mar. Chem.*, 78, 47–63, 2002.
- Hupe, A., and J. Karstensen, Redfield stoichiometry in Arabian Sea subsurface waters, *Global Biogeochem. Cycles*, 14, 357–372, 2000.
- Karl, D. M., and A. F. Michaels, Nutrient cycling: nitrogen cycle, in *Encyclopedia of Ocean Sciences*, edited by J. Steele, S. Thorpe, and K. Turekian, Academic, San Diego, Calif., 2001.

- Karl, D. M., J. R. Christian, J. E. Dore, D. V. Hebel, R. M. Letelier, L. M. Tupas, and C. D. Winn, Seasonal and interannual variability in primary production and particle flux at Station ALOHA, *Deep Sea Res., Part II*, 43, 539–568, 1996.
- Karl, D. M., K. M. Bjorkman, J. E. Dore, L. Fujieki, D. V. Hebel, T. Houlihan, R. M. Letelier, and L. M. Tupas, Ecological nitrogen-to-phosphorus stoichiometry at station ALOHA, *Deep Sea Res., Part II*, 48, 1529–1566, 2001a.
- Karl, D. M., R. R. Bidigare, and R. M. Letelier, Long-term changes in plankton community structure and productivity in the North Pacific Subtropical Gyre: The domain shift hypothesis, *Deep Sea Res., Part II*, 48, 1449–1470, 2001b.
- Laws, E. A., Photosynthetic quotients, new production and net community production in the open ocean, *Deep Sea Res.*, 38, 143–167, 1991.
- Li, Y. H., T. H. Peng, W. S. Broecker, and H. G. Oestlung, The average vertical mixing coefficient for the oceanic thermocline, *Tellus, Ser. B*, 36, 212–217, 1984.
- Li, Y. H., D. M. Karl, C. D. Winn, F. T. Mackenzie, and K. Gans, Remineralization ratios in the subtropical north Pacific gyre, *Aquat. Geochem.*, 6, 65–86, 2000.
- Minster, J., and M. Boulahdid, Redfield ratios along isopycnal surfaces: A complementary study, *Deep Sea Res.*, 34, 1981–2003, 1987.
- Morse, J. W., and F. T. Mackenzie, *Geochemistry of Sedimentary Carbonates*, 707 pp., Elsevier Sci., New York, 1990.
- Naqvi, S. W. A., D. A. Jayakumar, P. V. Narvekar, H. Naik, V. V. S. S. Sarma, W. D'Souza, S. Joseph, and M. D. George, Increased marine production of N₂O due to intensifying anoxia on the Indian continental shelf, *Nature*, 408, 346–349, 2000.
- Pahlow, M., and U. Riebesell, Temporal trends in deep ocean Redfield ratios, *Science*, 287, 831–833, 2000.
- Peng, T. H., and W. S. Broecker, C/P ratios in marine detritus, *Global Biogeochem. Cycles*, 1, 155–161, 1987.
- Redfield, A. C., The biological control of chemical factors in the environment, *Am. Sci.*, 46, 205–221, 1958.
- Sarmiento, J. L., J. C. Orr, and U. Siegenthaler, A perturbation simulation of CO₂ uptake in an ocean general circulation model, *J. Geophys. Res.*, 97, 3621–3645, 1992.
- Shaffer, G., Biogeochemical cycling in the global ocean, 2, New production, Redfield ratios, and remineralization in the organic pump, *J. Geophys. Res.*, 101, 3723–3745, 1996.
- Shaffer, G., J. Bendtsen, and O. Ulloa, Fractionation during remineralization of organic matter in the ocean, *Deep Sea Res., Part I*, 46, 185–204, 1999.
- Strous, M., J. A. Fuerst, E. H. M. Kramer, S. Logemann, G. Muyzer, K. T. Van De-Pas-Schoon, R. Webb, and J. G. Kuenen, Missing lithotroph identified as new planctomycete, *Nature*, 400, 446–449, 1999.
- Takahashi, T., W. S. Broecker, and S. Langer, Redfield ratio based on chemical data from isopycnal surfaces, *J. Geophys. Res.*, 90, 6907–6924, 1985.
- Troy, P. J., Y. H. Li, and F. T. Mackenzie, Changes in surface morphology of calcite exposed to the oceanic water column, *Aquat. Geochem.*, 3, 1–20, 1997.
- von Brand, T., N. W. Rakestraw, and C. E. Renn, The experimental decomposition and regeneration of nitrogenous organic matter in sea water, *Biol. Bull.*, 72, 165–175, 1937.
- Wanninkhof, R., S. Doney, T. H. Peng, J. L. Bullister, K. Lee, and R. A. Feely, Comparison of methods to determine the anthropogenic CO₂ invasion into the Atlantic Ocean, *Tellus, Ser. B*, 51, 511–530, 1999.
- Winn, C. D., Y. H. Li, F. T. Mackenzie, and D. M. Karl, Rising surface ocean dissolved inorganic carbon at the Hawaii Ocean Time-series site, *Mar. Chem.*, 60, 33–47, 1998.
- Yoshinari, T., Nitrous oxide in the sea, *Mar. Chem.*, 4, 189–202, 1976.
- Zhang, J. Z., C. W. Mordy, L. I. Gordon, A. Ross, and H. E. Garcia, Temporal trends in deep ocean Redfield ratios, *Science*, 289, 1839a, 2000.

Y.-H. Li, Department of Oceanography, University of Hawaii, Honolulu, HI 96822, USA. (yhli@soest.hawaii.edu)

T.-H. Peng, NOAA/AOML, Ocean Chemistry Division, Miami, FL 33149, USA. (Tsung-Hung.Peng@noaa.gov)